Application of laser-induced fluorescence for imaging sprays of model fuels emulating gasoline and gasoline/ethanol blends

M. Andersson[1*] and J. Wärnberg[2]
1) Department of Applied Mechanics, Chalmers University of Technology,
41296 Göteborg, Sweden
2) General Motors Powertrain – Sweden AB,
461 80 Trollhättan, Sweden

Abstract

The performance at cold start of spark-ignited car engines is still a challenge since slow and incomplete vaporization of the fuel causes high emissions of unburned hydrocarbons and may even cause difficulties to start at very low temperatures, in particular with alternative fuels such as ethanol. One approach to improve fuel evaporation is by direct injection into the cylinder late during the compression stroke. In this study the evaporation of fuel, including selective evaporation of fuel components of different volatility, has been studied, in sprays injected into air with a controlled pressure and temperature.

Planar laser-induced fluorescence (PLIF) and Mie scattering were used to image the fuel distribution in vapor and liquid phase in a cross-section of sprays. A model fuel of non-fluorescent molecules was used and a fluorescent tracer molecule was added. To simulate a fuel with a distillation curve similar to gasoline a multi-component model fuel was selected. The fuel was composed of five iso- or cyclo-alkenes with boiling points that span the 30-190°C range. As fluorescence tracers ketones: acetone, 3-pentanone and methylcyclohexanone, were used to trace light, medium-heavy and heavy fuel fractions. Besides investigating the gasoline-like model fuel, ethanol and an ethanol/multi-components fuel blend were investigated.

Spray imaging was carried out in a pressurized chamber. The injector was an outward-opening piezo-actuated injector generating a hollow-cone spray. A cross-section of the spray was illuminated by laser light at a wavelength of 266 nm formed into a thin sheet. Two intensified CCD-cameras were used to detect fluorescence and scattered light. The presence and penetration of liquid was determined by detecting Mie-scattered light. The PLIF-images provided the total distribution of fuel in liquid and vapor phase, and by comparing with the Mie-images it could be determined when the vapor started to appear in areas with little or no drops present indicating the presence of fuel vapor. It was found that at 90°C the light fuel components evaporated quickly, the medium-heavy components slowly while the heavy ones remained in liquid phase. At 140°C also the medium-heavy components evaporate relatively rapidly.

Introduction

There is today a demand for more fuel-efficient car engines and at the same time requirements for lower emissions both of species hazardous to health and of green-house gases. One approach to improve the efficiency of spark-ignited gasoline engines is to apply direct fuel injection. Direct injection enables the creation of a stratified fuel charge close to the spark plug, while operating the engine at globally lean conditions at low load reducing pumping and heat transfer losses and, thus, improving fuel efficiency and reducing CO_2 emissions [1]. Direct injection may also help reduce the emissions of unburned hydrocarbons during cold start.

The use of ethanol as a fuel for vehicles, in blends (E85 in Europe and USA) or neat as in Brazil is steadily gaining interest. Increased use of ethanol would decrease dependency on crude oil and decrease fossil carbon-dioxide emissions [2, 3]. Many manufacturers have products capable of ethanol use, so called flex-fuel vehicles [4], but they generally suffer from poor start ability at low ambient temperatures and must rely on block heaters beneath -15°C [5]. With the application of fuel direct injection and a stratified charge strategy this deficiency could be improved [6, 7]. The latest breed of direct injection systems, spray guided stratified combustion with piezo-actuated outward-opening nozzles could further improve the start ability because they deliver a very finely dispersed fuel cloud and are very precise in operation [1, 8]

[*]Corresponding author, f3cma@chalmers.se

In order to study the evolution of fuel-sprays at cold-start-like conditions, and in particular to which degree the fuel evaporates, we have imaged hollow-cone sprays from a piezo-actuated injector in a spray chamber at temperatures of 90-200°C. A cross-section of the spray was illuminated by a laser-light sheet and Mie-scattered light and fluorescence light was detected by CCD-cameras. To enable fluorescence imaging a non-fluorescent model fuel with lower and upper boiling points similar to those of commercial gasoline was used. Several different fluorescence tracers were added to the model fuel to indicate the distribution of fuel components of different volatility.

Table 1. Composition of the gasoline-like and ethanol-based model fuels without and with fluorescent tracers.

Compound	boiling point (°C)	MCF (% v/v)	MCF-ace (% v/v)	MCF-pent (% v/v)	MCF-mch (% v/v)	E100-but (% v/v)	E75-ace (% v/v)
isopentane	30	15	13	15	15		2.5
cyclopentane	50	15	12	15	15		
isooctane	99	45	45	40	45		11.25
cyclooctane	151	18	18	18	15		4.5
decalin	190	7	7	7	5		1.75
ethanol	78					95	75
acetone	56		5				5
2-butanone	80					5	
3-pentanone	101			5			
methylcyclohexanone	165				5		

Experimental Methods

Previously several model fuels have been used together with various fluorescent tracers in order to study the distribution of fuel components of different volatility [9-11]. Of these, the five-component fuel used by VanDerWege and Hochgreb [10] seems to be the combination that most closely follows the distillation curve of gasoline. That fuel contains two aromatic molecules, which is an advantage to achieve a fuel similar to gasoline since a significant fraction of commercial gasoline consists of aromatic molecules. Since light with a wavelength of 266 nm is used in this study, in contrast to VanDerWege and Hochgreb who used 308 nm, aromatic molecules are not suitable since they would absorb strongly at 266 nm. Instead cycloalkanes of similar boiling points were used. The composition of the undoped fuel is presented as multi-component fuel (MCF) in Table 1. Ethanol does not absorb at 266 nm and can be used directly, and for ethanol-gasoline blends a mixture of ethanol and MCF was used.

As fluorescent tracers ketones, which are popular tracer molecules due to a limited sensitivity to quenching by oxygen [12], were chosen. Furthermore, ketones are available with boiling points almost spanning the distillation curve of gasoline, starting with acetone with a boiling point of 56°C at 1 bar. Acetone (ace) was used to trace the light fraction of the fuel. Two other ketones, 3-pentanone (pent) and methylcyclohexanone (mch), were used to trace the medium-heavy and heavy components respectively, and 2-butanone (but) was used to trace ethanol. Ketones were added in a concentration of 5 % replacing base fuel molecules of similar volatility as described in Table 1.

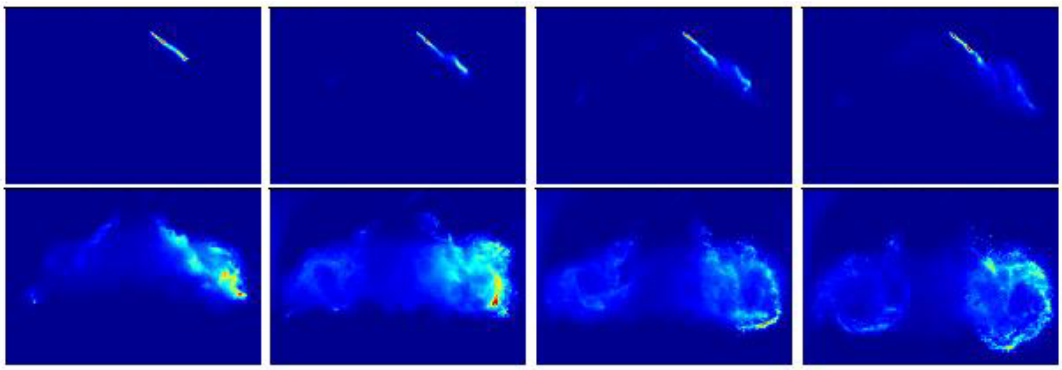

Figure 1. Images of Mie-scattered light recorded at a 140°C and 6.8 bar with MCF-pent as fuel. In the first row the images are recorded 0.2, 0.3, 0.4 and 0.5 ms asoi, and in the second row 0.6, 0.8, 1.0 and 1.3 ms asoi. The maximum intensity in the upper row is about 7 times higher than in the lower row and the false color scale is adjusted accordingly. The image size is 35x50 mm.

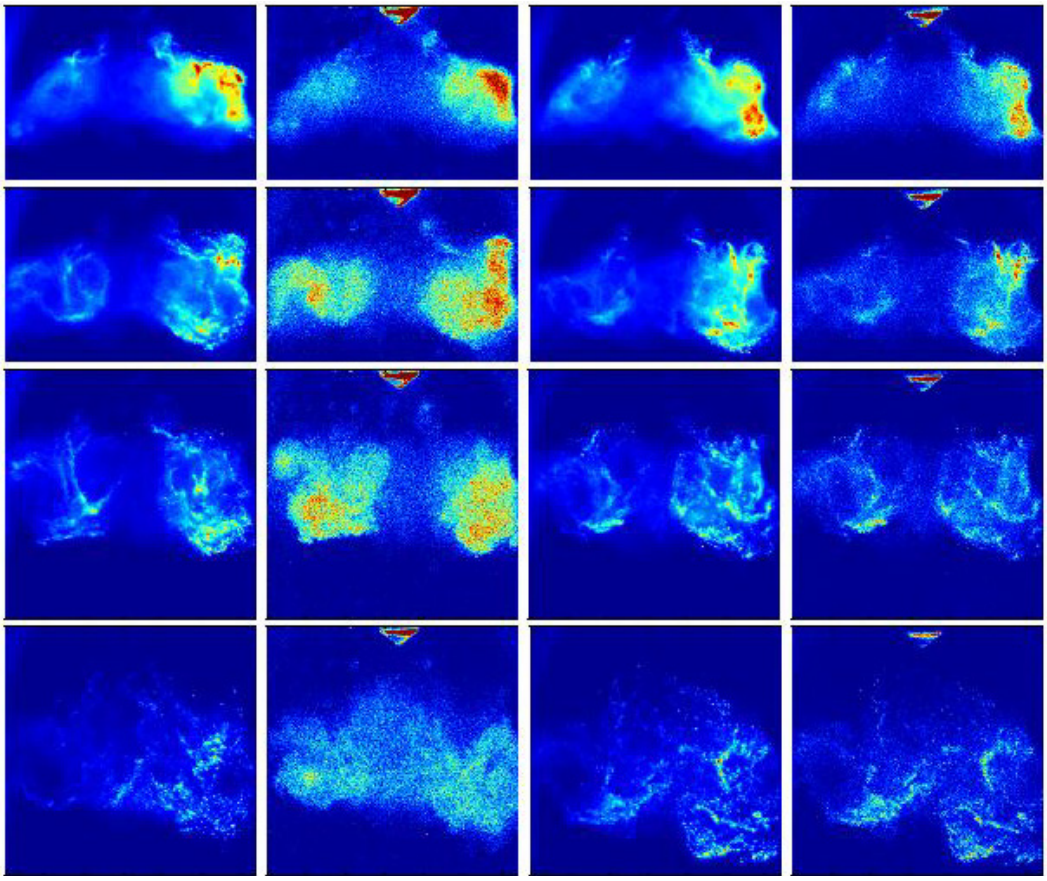

Figure 2. Image pairs of sprays recorded at a 90°C and 6 bar. The two left columns are recorded with MCF with acetone as the tracer, and the two right columns are recorded with methylcyclohexanone as the tracer. Columns 1 and 3 are images of Mie-scattered light, and columns 2 and 4 are LIF images recorded simultaneously as the Mie-images in column 1 and 3 respectively. The rows show, from top to bottom, images recorded 0.9, 1.5, 2.3 and 4.2 ms asoi. The image size of row 1 and 2 is 35x50 mm and row 3 and 4 50x50 mm.

The spray imaging was carried out in Chalmers high-pressure/high-temperature spray chamber. It is a constant-pressure chamber through which air flows continuously. The air is heated before entering the chamber and the temperature is measured by a thermocouple in the chamber. The chamber has large quartz windows, 125 mm high 48 mm wide, for laser-light to pass and for imaging. The fuel injector is mounted from the top of the chamber. The injector mount is cooled by water, but the temperature of the injector cannot be exactly controlled and may vary with the chamber temperature. The injector is a piezo-actuated outward-opening injector generating a hollow-cone spray. In the present study, a fuel pressure of 200 bar was applied and the injection duration was 0.4 ms.

For excitation the fourth harmonic light from a Nd:YAG-laser with a wavelength of 266 nm was used. The light was formed into a 50 mm high sheet passing just under the injector. Images were recorded perpendicularly to the laser plane. Due to the limited size of the window the full width of the spray could not be imaged. Two intensified CCD-cameras were used for the imaging. A dichroic mirror reflected light at 266±25 nm towards one of the cameras, with a band-pass filter transmitting 265±12 nm, detecting Mie-scattered light. The fluorescence light was transmitted through the dichroic mirror and detected by the other camera with a long-pass filter, WG360, in front.

Results and Discussion

Measurements were carried out with the multi-component fuel with three different tracers. For each fuel composition measurements were carried out at three different temperatures, 90, 140 and 200°C, of the air in the spray chamber, selected to represent conditions that could occur during cold start of a spark-ignited engine. The air pressure was 6.0, 6.8 and 7.8 bar, respectively, in order to have a similar air density and spray penetration in the three cases. Images were recorded from the start of the injection up to 10 ms after start of injection (asoi).

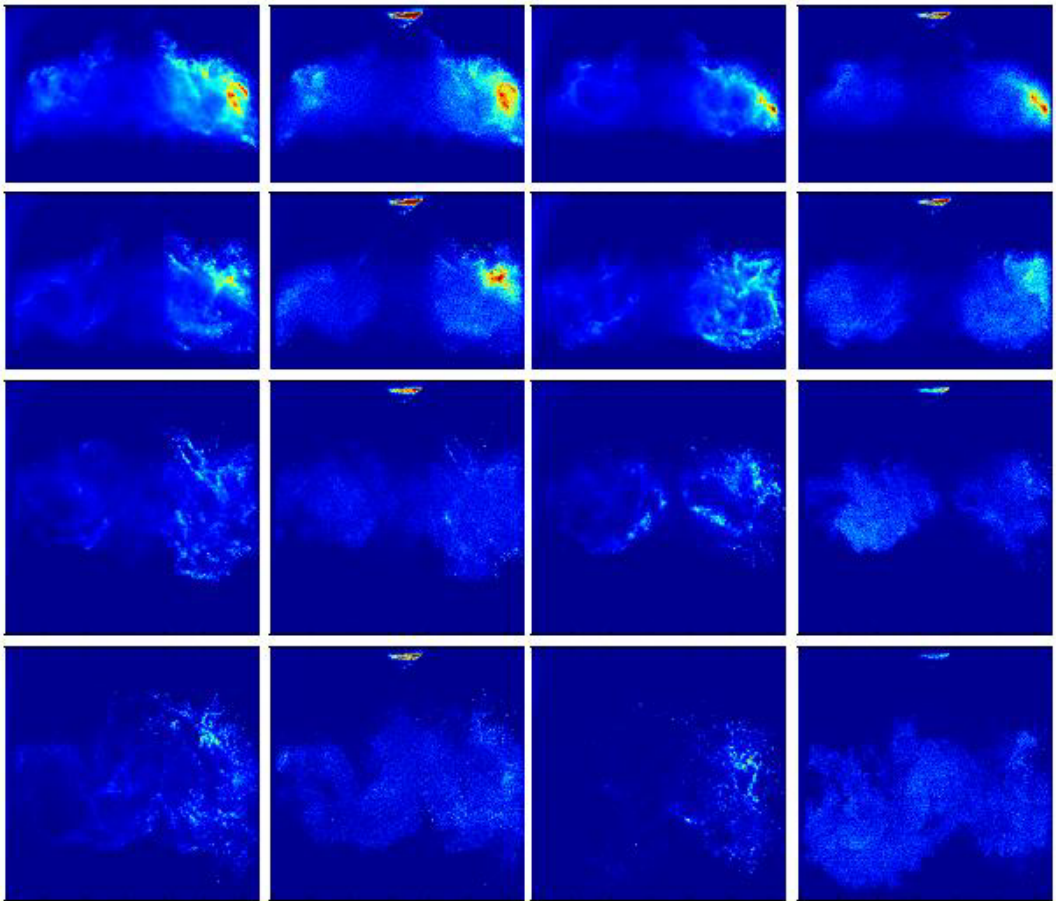

Figure 3. Image pairs of sprays of MCF with 3-pentanone as tracer. The two left columns are recorded at 90°C and 6 bar, and the two right columns are recorded 140°C and 6.8 bar. Columns 1 and 3 are images of Mie-scattered light, and columns 2 and 4 are LIF images recorded simultaneously as the Mie-images in column 1 and 3 respectively. The recording times and image sizes are the same as in Fig. 2.

The main features of the spray development can be described based on the images of Mie-scattered light as shown in Fig 1. The hollow cone is formed and appears as a thin layer. Already after 0.3 ms asoi there is an indication of vortex formation seen as a sudden increase in the cone diameter. During this initial part of the imaging, while the fuel is still being injected, there is a very strong scattering and attenuation of the incoming laser light. Only the right side of the spray, from where the laser light sheet enters, becomes illuminated. During the next millisecond the vortices are further developed at the bottom of the cone, and the fuel is only slowly propagating in the vertical direction. The initial cone and vortex formation is very similar for the three temperatures, but at later times than shown in Fig. 1 the different evaporation rates lead to different characteristics.

In order to analyze if and when the fuel evaporates and how the fuel vapor is distributed compared to the liquid fuel, LIF-images are compared to the simultaneously recorded Mie-images. Mie scattering from the drops is orders of magnitude stronger than Rayleigh scattering from fuel vapor so it can be assumed that the elastically scattered light only originates from parts of the spray containing drops, whereas the tracer molecules fluoresce both in liquid and vapor phase. The analysis is a qualitative analysis based on inspecting a large number of image pairs where details, not observable in averaged images, can be seen. Here only a selection of representative images can be shown.

Fig. 2 shows image pairs (simultaneously recorded Mie and LIF images) of sprays of MCF with acetone and methylcyclohexanone as tracers recorded at 90°C. The Mie and LIF images of MCF-mch are very similar, showing not only an over all similar structure, but also details of fuel distribution agrees well between the two images. From this can be concluded that fluorescence is only observed from the same points as there are liquid drops and, thus, that the heavy fuel components remain in liquid phase during the observation time. In contrast, a discrepancy between Mie and LIF images of MCF-ace starts to appear already 0.9 ms asoi. In the Mie-image an area of lower in-

tensity is seen at the center of a vortex on the left side, whereas a relatively high intensity is detected at the corresponding spot in the LIF image. The evaporation is however far from complete since the structures with the highest intensity in the Mie images are also clearly seen in the LIF images. At later times, several of the voids (likely centers of vortices) seen in the Mie images, correspond to maxima in the fuel concentration in the LIF images. Thus, the vapor of the more volatile components appears to move towards the center of the vortices.

When the medium heavy components, traced by 3-pentanone, are followed the behavior is between that of the light and heavy components. As can be seen in Fig. 3 there is at 90°C not much difference between the Mie and LIF-images initially, only from 1.5 ms asoi discrepancies between the Mie- and LIF-images can be seen, where voids in the drop structure start to be filled by vapor. However, at least till 2.3 ms asoi the main structures of the drop distribution can be recognized also in the LIF-images showing that a significant fraction of the medium heavy components still remains in the drops. At 140°C the evaporation is more rapid. This can be seen as a more rapid filling of the voids in the drop structure, and at the later times, the streaks of high intensity in the Mie-images cannot be recognized in the LIF-images signaling that the medium-heavy components already have evaporated. The total intensity of the Mie signal has also decreased, indicating that only a small fraction of the fuel still remains in liquid phase.

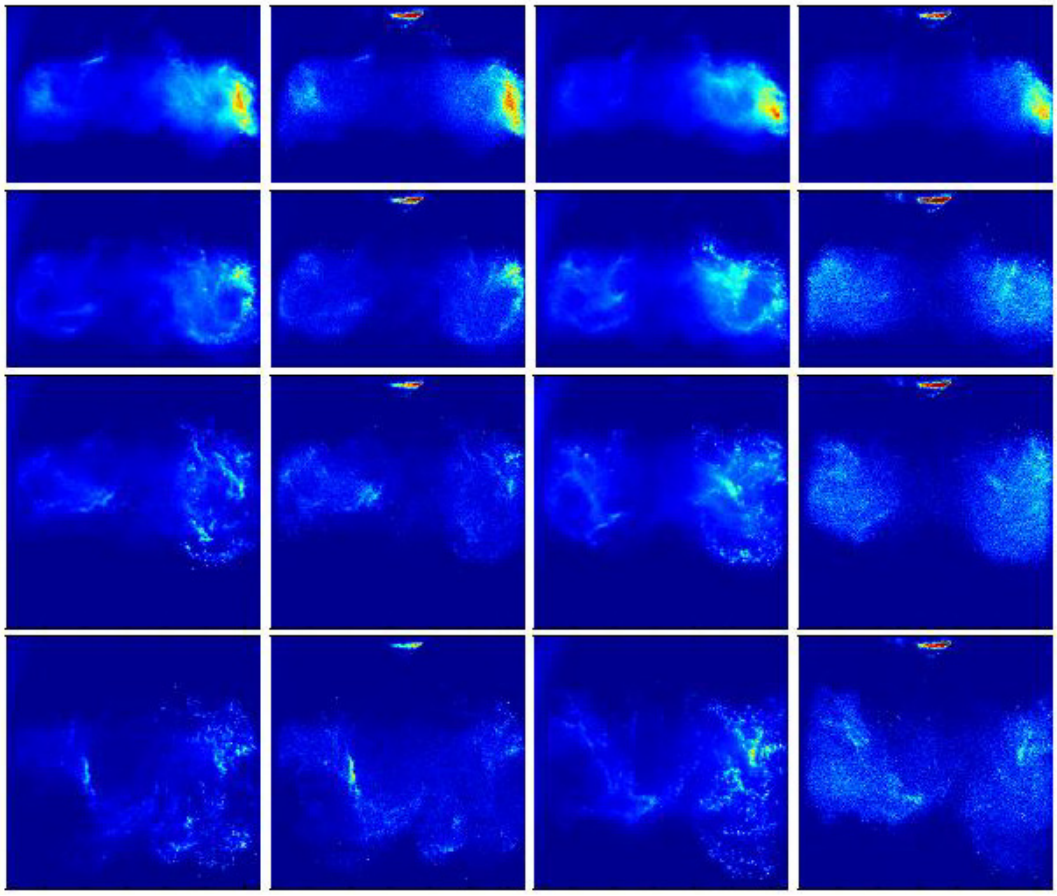

Figure 4. Image pairs of sprays recorded at 90°C and 6 bar. The two left columns are recorded with E100 with 2-butanone as the tracer, and the two right columns are recorded with E75 with acetone as the tracer. Columns 1 and 3 are images of Mie-scattered light, and columns 2 and 4 are LIF images recorded simultaneously as the Mie-images in column 1 and 3 respectively. The recording times and image sizes are the same as in Fig. 2.

In addition to the gasoline-like fuels, sprays of pure ethanol and E75 were investigated. The reason for using E85 (E75 during winter) in northen Europe is to improve cold start performance. Therefore, acetone was used as a tracer in E75 to investigate if the lighter fuel components of the gasoline fraction evaporate faster than the ethanol at the conditions employed here. Fig. 4 shows images of sprays of E100-but and E75-ace. It is indeed so that indications of vapor appearing outside the drop distribution are first observed for E75-ace. However, it is not until about

1.5 ms asoi that there is a clear difference in the fuel distribution between the Mie- and LIF-images and a filling of the vortices, although the fuel distribution in the LIF-images is somewhat more diffuse already slightly earlier. For E100-but clear differences show up even later, with some indications of a more smooth fuel distribution in the LIF-image 2.3 ms asoi, but the fact that the structure of the drop distribution is dominating the LIF images shows that a large fraction of the fuel is still in liquid phase.

The acetone appears to evaporate and diffuse much slower from E75 than from MCF. This may be due to the higher heat capacitivity and heat of vaporization of ethanol compared to the alkanes. The air-fuel mixing in the spray may also be different, since the vortex structure in the Mie images is not so pronounced for the ethanol fuels as for MCF (compare Mie-images of Figs 2 and 4). This is in agreement with observations by Hemdal et al. [13], who found a weaker and more compact vortex structure, as well as larger drop diameters, for ethanol.

In all cases where evaporation is observed the vapor penetrates "inwards" to fill voids in the vortex structure created by the streams of droplets. There is no significant amount of vapor observed outside the borders of the liquid phase until the drops disappear by evaporation. This means that this type of injector enables the creation of a stratified fuel charge that is confined by the vortices created. On the other hand, while there are still liquid drops present there is no significant volume with only fuel vapor. The observation that the vapor is confined to the volume created by the vortices means that methods such as high-speed imaging of scattered white light of fuel drops provide results that are relevant for predicting the distribution also of vapor phase fuel [13].

Conclusions

A five-component model fuel with ketone tracers of different boiling points has successfully been applied to image the vapor-phase distribution of fuel components of different volatility using LIF and Mie-scattering. Comparisons between LIF and Mie images show that there is a selective evaporation of lighter fuel components at air temperatures of 90 and 140°C, i.e. temperatures that are encountered at cold-start conditions. This is in contrast to results from an engine study carried out at normal operating conditions where the distribution of light and heavy components appeared similar, which was explained by that the evaporation rate was faster than the diffusion rate inside the drops [14]. The evaporation from E75 and in particular pure ethanol appears slower than from MCF for components of the same volatility. It was observed that the fuel vapor fills the voids in the vortex structure formed by the spray drops, but does not significantly penetrate beyond the borders of the volume filled by the drops.

Acknowledgements

Financial support from the Combustion Engine Research Centre (CERC) at Chalmers is gratefully acknowledged by MA.

References

1. Baecker, H., Kaufman, A., Tichy, M., *SAE Technical Paper*: 2007-01-1407 (2007).
2. Farell, A. E., Plevin, R. J., Turner, B. T., Jonas, A.D., O'Hare, M., Kammen, M., *Science* 311: 506-508 (2006).
3. www.baff.info (as of 2008-09-16).
4. West, B. H., López, A. J., Theiss, T. M., Graves, R. L., Storey, J. M., Lewis, S. A., *SAE Technical Paper:* 2007-01-3994 (2007)
5. Hauet, B., Grand, JG., Jouron, C., Tran-Dinh, C., *International conference INSA de Strasbourg*, Strasbourg, France, November 2007.
6. Bäcker, H., Tichy, M., Achleitner, E., Pischinger, S., Lang, O., Habermann, K., Krebber-Hortmann, K., *Direkteinsprizung im Ottomotor VI*, Expert verlag, 2007, pp. 238-252.
7. Kapus, P. E., Fuerhapter, A., Fuchs, H., Fraidl, G. K., *SAE Technical Paper*: 2007-01-1408 (2007).
8. Dahlander, P., Gutkowski, A., Denbratt, I., *22nd European Conference on Liquid Atomization and Spray Systems*, Como, Italy, September 2008, ILASS08-A129 (2008).
9. Krämer, H. Einecke, S., Schulz, Ch., Sick, V., Nattrass, S.R., and Kitching, J.S., *SAE Technical Paper:* 982467 (1998).
10. VanDerWege, B.A. and Hochgreb, S., *SAE Technical Paper:* 2000-01-0535 (2000).
11. Styron, J.P. Kelly-Zion, P.L., Lee, C.F., Peters, J.E., White, R.A., and Lucht, R.P., *SAE Technical Paper:* 2000-01-0243 (2000).
12. Schulz, C. and Sick, V., *Prog. Energy Combust. Sci.* 31: 75-121 (2005).
13. Hemdal, S. Wärnberg, J. Denbratt, I., Dahlander, P., *SAE Technical Paper*: 2009-01-1496 (2009).
14. Zhang, R. and Sick. V., *SAE Technical Paper*: 2007-01-1826 (2007).